The new isotope ^{179}Pb and α-decay properties of ^{179}Tl ^{m}

2010 J. Phys. G: Nucl. Part. Phys. 37 035102

(http://iopscience.iop.org/0954-3899/37/3/035102)

J. Phys. G: Nucl. Part. Phys. **37** (2010) 035102 (10pp) doi:10.1088/0954-3899/37/3/035102

The new isotope ^{179}Pb and α-decay properties of ^{179}Tl^m

A N Andreyev[1,2], S Antalic[3], D Ackermann[4], T E Cocolios[2], V F Comas[4], J Elseviers[2], S Franchoo[5], S Heinz[4], J A Heredia[4], F P Heßberger[4], S Hofmann[4,6], M Huyse[2], J Khuyagbaatar[4], I Kojouharov[4], B Kindler[4], B Lommel[4], R Mann[4], R D Page[7], S Rinta-Antila[7], P J Sapple[7], Š Šáro[3], P Van Duppen[2], M Venhart[2] and H V Watkins[7]

[1] School of Engineering and Science, University of the West of Scotland, Paisley, PA1 2BE, UK
[2] Instituut voor Kern- en Stralingsfysica, K.U. Leuven, University of Leuven, B-3001 Leuven, Belgium
[3] Department of Nuclear Physics and Biophysics, Comenius University, Bratislava, SK-84248, Slovakia
[4] GSI Helmholtzzentrum für Schwerionenforschung GmbH, 64291 Darmstadt, Germany
[5] IPN Orsay, F-91406 Orsay Cedex, France
[6] J.W. Goethe-Universität, D–60054 Frankfurt, Germany
[7] Department of Physics, Oliver Lodge Laboratory, University of Liverpool, Liverpool L69 7ZE, UK

E-mail: Andrei.Andreyev@uws.ac.uk

Received 13 November 2009
Published 22 January 2010
Online at stacks.iop.org/JPhysG/37/035102

Abstract
The new isotope ^{179}Pb has been produced in the complete fusion reaction ^{40}Ca+^{144}Sm $\rightarrow$ ^{179}Pb+5n at the velocity filter SHIP (GSI). Its α-decay energy of 7350(20) keV and half-life value of $3.5^{+1.4}_{-0.8}$ ms were deduced based on the recoil–α–α correlation technique. A spin parity of $I^\pi = (9/2^-)$ was tentatively assigned to the ground state of ^{179}Pb; thus, it is based on the $1h_{9/2}$ orbital. Improved measurements of the α-decay properties of ^{179}Tl^m and ^{175}Au^m are also presented.

1. Introduction

The odd-A neutron-deficient isotopes $^{183-189}$Pb are well known for the systematic appearance of two α- and/or β-decaying states with spin and parity assignments of $I^\pi = 3/2^-$ for the ground state and of $13/2^+$ for the isomeric state [1, 2]. These states are produced when an odd valence neutron occupies either the $3p_{3/2}$ or the $1i_{13/2}$ spherical orbitals, respectively. Recent laser spectroscopic studies at the mass separator ISOLDE confirmed these conclusions by measuring the magnetic moments and charge radii of both the $3/2^-$ ground state and the $13/2^+$ isomer in the isotopes $^{183-189}$Pb [2–4]. A surprising observation for all these isotopes was the persistence of the $3/2^-$ ground state even down to the neutron number $N = 101$ (^{183}Pb), despite the fact that in the spherical shell model the $3p_{3/2}$ orbital should already become empty by

$N = 114$ (^{196}Pb). Within the shell model it would be expected that below the neutron mid-shell at $N = 104$, the $1h_{9/2}$ or $2f_{7/2}$ neutron orbitals should become important in the Pb isotopes, as in the lightest Pt and Hg isotopes [1, 5].

Consistent with this expectation, recent α-decay study of ^{181}Pb [6, 7] showed that for the first time in the Pb isotopes, an α-decaying state with $I^{\pi} = (9/2^{-})$ was observed in this isotope. The change of the ground state spin in ^{181}Pb relative to the heavier odd-A Pb isotopes is believed to be due to the complete depletion of the $i_{13/2}$ and $p_{3/2}$ orbitals lying above the $N = 100$ spherical sub-shell closure and a creation of a hole in the $h_{9/2}$ spherical orbital lying below this gap. No unambigous evidence for the $3/2^{-}$ or $13/2^{+}$ states has been observed in ^{181}Pb in our study [7], but a possible decay from a $13/2^{+}$ state was briefly mentioned in [6].

The present work extends these studies to the even lighter isotope ^{179}Pb, which was identified for the first time in our experiment at the velocity filter SHIP (GSI, Darmstadt) [8, 9].

2. Experimental set-up

The method used in this work was described in detail in our study of ^{181}Pb [7]; thus, only a description of the most relevant features will be given here.

The new isotope ^{179}Pb was produced in the complete fusion reaction ^{40}Ca+^{144}Sm $\rightarrow$ ^{179}Pb+5n. The typical intensity of the ^{40}Ca beam, provided by the UNILAC of GSI, was 400 pnA. Most of the data were collected at a beam energy of 232 MeV in front of the target, corresponding to the maximum of the 5n evaporation channel of the studied reaction.

Eight ^{144}Sm targets, each of 96.4% isotopic enrichment and 350 μg cm^{-2} thickness, were mounted on a wheel, rotating synchronously with the UNILAC macro-pulsing. The targets were produced by evaporating the $^{144}SmF_3$ material onto a carbon backing of 40 μg cm^{-2} thickness.

After separation by the velocity filter SHIP, the evaporation residues (ERs) were implanted into a 300 μm thick, 35 $\times$ 80 mm^2 16-strip position-sensitive silicon strip detector (PSSD), where their subsequent particle decays were measured by using standard implantation and correlation techniques [9].

The α-particle energy calibration of the PSSD was performed by using known α lines of the isotopes $^{176-182}$Hg (and their daughters), produced via α, xn channels in the studied reaction. The broad energy range of $\sim$5300–6800 keV and a small energy uncertainty for most of the α lines used for the calibration allowed us to make a reliable calibration extrapolation in the α-energy region of 7200–7400 keV, relevant for ^{179}Pb and ^{179}Tl^{m}. A typical PSSD energy resolution of $\sim$25 keV (FWHM) was achieved in the energy interval of 6000–7500 keV for full-energy α decays measured in the PSSD. The position resolutions of 0.35 mm (FWHM) and 0.25 mm (FWHM) for ERs–alpha and alpha–alpha correlation analyses were achieved, respectively. Since α emission is a dominant decay mode in most of the nuclei produced in this reaction, the identification of nuclides was based on the observation of genetically correlated α-decay chains complemented with excitation function measurements.

A large-volume 4-fold segmented Clover germanium detector was installed behind the PSSD to measure the energies of γ rays occurring within 5 μs after the detection of any particle in the PSSD. The energy threshold for the γ-rays registration was at $\sim$15 keV; therefore, we could not observe Hg L x rays ($E_{\gamma} \sim$ 9–12 keV) in this experiment.

Upstream of the PSSD, six silicon detectors of similar shape were mounted in an open box geometry, see details in [10]. These 'BOX detectors' were used to measure the energies of the particles (α particles and conversion electrons), escaping from the PSSD in the backward direction. By adding up the energy deposition in the PSSD and BOX detectors, after accounting

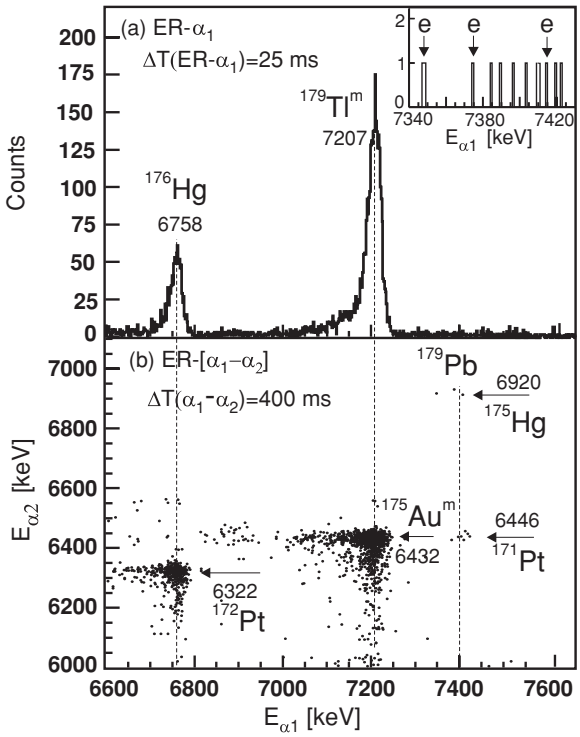

Figure 1. (a) Part of the α_1-energy spectrum from the reaction ^{40}Ca+^{144}Sm $\rightarrow$ ^{184}Pb* registered within 25 ms after the ER implantation in the PSSD. Alpha-decay energies are given in keV. The inset shows the energy spectrum of 12 correlated α_1 events assigned to the α decay of ^{179}Pb. The positions of three escaped (but reconstructed 'PSSD+BOX') α_1 decays are marked by an arrow with a symbol 'e' (see the text for details); (b) the α_1–α_2 correlation plot for the α_1 decay from the panel (a), measured within the time interval of $\Delta T\,(\alpha_1\text{-}\alpha_2) \leqslant 400$ ms. Only the α decays with the full energy deposition in the PSSD were considered for this spectrum, see the text for details.

for the energy loss in the 'dead' layers of both detectors, the full energy of the escaping α particles could be recovered, though with a somewhat reduced energy resolution. A typical α-energy resolution for the sum signal was $\sim$70 keV (FWHM), which was in most cases sufficient to distinguish the decays of interest unambiguously. We note that this method was used only for three 'escape' events of ^{179}Pb (see the next section).

Three time-of-flight (TOF) detectors [11] were installed in front of the BOX+PSSD system allowing us to distinguish the reaction products from the scattered beam particles. In addition, decay events in the PSSD could be distinguished from the implantation events by requiring an anticoincidence condition between the signals from the PSSD and from at least one of the TOF detectors.

3. Experimental results

3.1. New isotope ^{179}Pb

Figure 1(a) shows a part of the energy spectrum of α decays collected during the time interval of 25 ms after the ER implantation in the PSSD at the beam energy of 232 MeV. The two prominent peaks are due to α decay of ^{179}Tl^m (see the next section) and of ^{176}Hg, produced via the p4n and α4n evaporation channels, respectively. Figure 1(b) shows a two-dimensional plot

of α_1–α_2 correlations for the time interval of $\Delta T\,(\alpha_1$–$\alpha_2) \leqslant 400$ ms. The two strongest groups of known α_1–α_2 correlations due to ^{176}Hg–^{172}Pt and ^{179}Tl^m–^{175}Au^m (see the next section) are marked in the spectrum.

From a comparison of the intensity of the ER–α_1(^{176}Hg) correlation group in figure 1(a) with that of the ER–α_1(^{176}Hg)–α_2(^{172}Pt) group in figure 1(b), an α-decay branching ratio of $b_\alpha = 97(3)\%$ was deduced for ^{172}Pt. This value is consistent with but is more precise than the values of $b_\alpha = 94^{+6}_{-32}\%$ from [12] and $b_\alpha = 94(12)\%$ from [13].

The new isotope ^{179}Pb was identified by correlations of its α decays with the α decays of its known daughter and grand-daughter products ^{175}Hg ($E_\alpha = 6913(5)$ keV, $T_{1/2} = 10(1)$ ms [14]) and ^{171}Pt ($E_\alpha = 6453(3)$ keV, $T_{1/2} = 44(7)$ ms [1]), respectively. In particular, three events of the type ER–α_1(^{179}Pb)–α_2(^{175}Hg(6920(20) keV)) and seven events of the type ER–α_1(^{179}Pb)–α_2(^{171}Pt(6446(15) keV)) have been observed in figure 1(b). Both the decay energies and half-life values for the daughter isotopes match well the published data and will not be discussed further. In total nine decay events of ^{179}Pb were observed in figure 1(b). One of these correlated decay chains was of the type ER–α_1(^{179}Pb)–α_2(^{175}Hg)–α_2(^{171}Pt). This is consistent, within the limited statistics available, with the expected number of 2.7 for such correlation chains, if one takes into account the PSSD efficiency of ∼55% for the registration of the full-energy α decays.

Additionally, by using the BOX detectors, a search was made for the 'escaping' α particles. This increased the number of registered correlated decay events of ^{179}Pb up to 12, though at the expense of a somewhat reduced energy resolution for the three 'reconstructed' escaping α decays. The α_1-energy spectrum of all 12 correlated events is shown in the inset to figure 1(a), in which the positions of three reconstructed 'PSSD+BOX' events are shown by the arrows with a symbol 'e'. The mean value of this spectrum is 7394(30) keV, but the events span the energy interval of 7347–7423 keV, which is at least twice as broad as, e.g., the energy distribution of the single peaks at 6758 keV and 7207 keV in figure 1(a). We also stress here that only one of the two lowest energy events at ∼7348 keV in figure 2 is a recovered 'PSDD+BOX' event. Therefore, the conclusion regarding the broad energy distribution of the α decays of ^{179}Pb will still be valid even if only nine full energy events from figure 1(b) are considered. No γ rays have been observed in coincidence with these 12 α decays of ^{179}Pb.

The meaning of all these observations and the deduced decay scheme of ^{179}Pb will be discussed in section 4.1.

The half-life value of $T_{1/2}(^{179}\text{Pb}) = 3.5^{+1.4}_{-0.8}$ ms was deduced by using the data for the 12 correlated events.

The production cross section of $\sigma(^{179}\text{Pb}) = 140(40)$ pb was deduced at a beam energy of 232 MeV, by assuming the calculated SHIP efficiency of 40% for this reaction. The quoted uncertainty is due to statistics only.

3.2. $^{179}Tl^m \rightarrow {}^{175}Au^m$ decay

A similar correlation analysis was performed for the short-lived isomer ^{179}Tl^m (see figure 1). In our experiment we obtained approximately 3000 ER–α_1(7207 keV) correlations, which is more than an order of magnitude larger than in any of the previous experiments reporting data on this isomer [15–18]. Thus, more precise values of $E_\alpha = 7207(5)$ keV and $T_{1/2} = 1.46(4)$ ms (see figure 2) have been deduced for ^{179}Tl^m. Our data are compared to the previously reported data in table 1.

We note that based on a limited number of observed decays (a few counts only, see figure 2 of [17]), a second α decay with $E_\alpha = 7096(10)$ keV, $T_{1/2} = 1.6(8)$ ms, $I_\alpha = 20(9)\%$ was assigned to ^{179}Tl^m in the study [17] in addition to the 'main' 7213(10) keV α decay. As

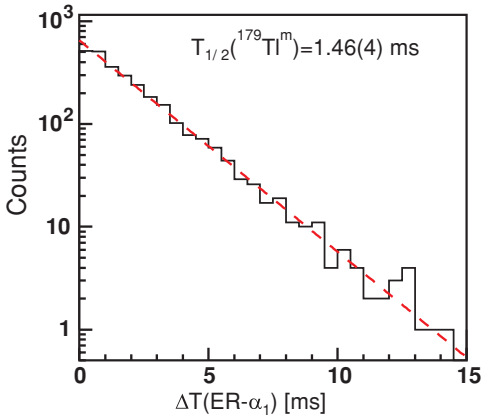

Figure 2. The time distribution between the ER implantations and the subsequent 7207 keV α decays of $^{179}Tl^{m}$ from figure 1(a). The exponential fit is shown by the red dashed line.

(This figure is in colour only in the electronic version)

Table 1. A comparison of α-decay energies E_α and half-life values $T_{1/2}$ for $^{179}Tl^{m}$ from our measurement and from the earlier data.

E_α, keV	$T_{1/2}$(ms)	Reference
7207(5)	1.46(4)	Present work
7200(20)	1.4(5)	[15]
7201(20)	$0.7^{+0.6}_{-0.4}$	[16]
7213(10)	1.8(4)	[17]
7201	1.7(2)	[18]

suggested in [17], this fine-structure α decay would presumably feed to an excited state at $\sim$120 keV above the state in ^{175}Au fed by the 7213 keV decay. However, no such state has been seen in the recent in-beam study of ^{175}Au [19]. Consistent with this and despite approximately 2 orders of magnitude larger statistics for $^{179}Tl^{m}$ in our study than in [17], no evidence for the 7096 keV α decay has been observed in our experiment with the upper intensity limit for this line of 3% relative to the 7207 keV peak, see figure 1. The weak low-energy tails of peaks at 6758 keV and 7207 keV in figure 1 are most probably both due to the radiation damage of the PSSD used in this experiment. Also, we did not observe any α–γ coincidences which could be attributed to the decay of $^{179}Tl^{m}$.

Our measured α-decay energy $E_\alpha = 6432(5)$ keV and half-life value of $T_{1/2} = 138(5)$ ms for ^{175}Au are in good agreement with the values $E_\alpha = 6.43$ MeV and $T_{1/2} = 143(8)$ ms reported in [19]. In the following we will denote the group belonging to ^{175}Au as '$^{175}Au^{m}$' due to the reasons discussed below.

From the comparison of the intensities of the ER–$\alpha_1(^{179}Tl^{m})$ correlation group in figure 1(a) and of the ER–$\alpha_1(^{179}Tl^{m})$–$\alpha_2(^{175}Au^{m})$ group in figure 1(b), an α-decay branching ratio of $b_\alpha = 90(3)\%$ was deduced for $^{175}Au^{m}$. This value is consistent with but is more precise than the value of $b_\alpha = 94^{+6}_{-25}\%$ from the work reported in [15].

The decay sequence of the isotope $^{179}Tl^{m}$ as deduced from our ER–α–α correlation analysis is shown in figure 3. To enhance the correlations due to the short-lived $^{179}Tl^{m}$ and also allow the correlations with the longer lived daughter nuclides, the analysis was

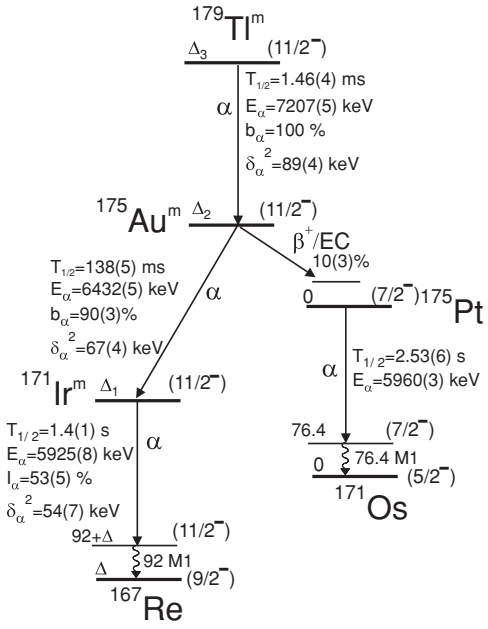

Figure 3. Decay sequence starting from ^{179}Tl^{m} deduced in our work. Our measured data for ^{179}Tl^{m}, ^{175}Au^{m} and ^{171}Ir^{m} are shown, except for the evaluated half-life of ^{171}Ir^{m}, which is taken from [1]. The data for ^{171}Ir^{m} and ^{175}Pt, relevant for this work, are taken from [1]. The excitation energies of the $(11/2^{-})$ isomeric states in ^{179}Tl, ^{175}Au and ^{171}Ir and of the $(9/2^{-})$ state in ^{167}Re relative to the respective ground states in these nuclei (not shown in the figure) are not known and are denoted by the symbols Δ_3, Δ_2, Δ_1 and Δ, respectively. All I^{π} assignments are tentative and shown in brackets. The reduced α-decay widths δ_{α}^{2} have been calculated with the assumption of $\Delta L = 0$, following the Rasmussen prescription [20]. The β^{+}/EC-decay branch of ^{175}Au^{m} toward excited states in ^{175}Pt is shown schematically, see discussion in section 4.2. Gamma-ray energies are given in keV.

performed with the following conditions: $\Delta T(\text{ER}–\alpha_1) \leqslant 5$ ms, $\Delta T(\alpha_1–\alpha_2) \leqslant 8$ s. The first condition effectively suppressed the contributions of the longer lived parent isotopes produced in the reaction. To our knowledge, this is the first time that the complete correlated decay chain from ^{179}Tl^{m} to its daughter products ^{167}Re and ^{171}Os has been unambiguously seen in a data analysis. In particular, in the correlation analysis we were able to clearly see the α(5925 keV)–γ(92 keV) and α(5960 keV)–γ(76.4 keV) coincident events due to the decays of ^{171}Ir^{m} and ^{175}Pt, respectively, see the decay scheme in figure 3. It is also worth to mention, that the relative position of the high-spin $(9/2^{-})$ and the low-spin isomers in ^{167}Re is not known; thus, it is not clear which one of them is the ground state, see discussion in [1].

From the comparison of the intensities of the ER–α_1(^{179}Tl^{m})–α_2(^{175}Au^{m}) and ER–α_1(^{179}Tl^{m})–α_2(^{171}Ir^{m}) correlations an α-decay branching ratio of $b_{\alpha} = 53(5)$ % was deduced for ^{171}Ir^{m}. This value is consistent with but is more precise than the value of $b_{\alpha} = 58(11)$% from [16].

Finally, we note that in this experiment we also collected data for the decay of the ground state of ^{179}Tl. However, the correlation analysis for ^{179}Tl^{g} was hampered by its longer half-life value of $T_{1/2} = 230(40)$ ms [17], by the similarity of the decay properties of its decay products to the daughter products of ^{179}Tl^{m} and by a large number of background nuclides produced in the reaction. On the other hand, the decay sequence of ^{179}Tl^{g} was recently studied in a

separate experiment at the mass separator ISOLDE [21]. The uniqueness of this experiment was that the shorter lived ^{179}Tl^{m} was not extracted from the target of ISOLDE (due to the much longer release time); thus, a very pure, mass-separated source of ^{179}Tl^{g} was available in this experiment. Therefore, the detailed discussion of the decay sequence of ^{179}Tl^{g} will be given elsewhere [21].

4. Discussion

4.1. ^{179}*Pb* α *decay*

Our explanation of the broad energy distribution (E_α = 7347–7423 keV, see the inset to figure 1(a)) of the 12 α-decay events assigned to ^{179}Pb is based on a recent in-beam study of ^{175}Hg [14]. There, a low-lying $(9/2^-)$ state at E^* = 80 keV was identified, which decays by an 80 keV $M1$ transition to the presumed $(7/2^-)$ ground state. A similar situation is also known in ^{177}Hg [22], in which a low-lying $(9/2^-)$ state at E^* = 77 keV decays by a 77 keV $M1$ transition to the presumed $(7/2^-)$ ground state.

The 80 keV $M1$ transition in ^{175}Hg has a total conversion coefficient of $\alpha_{\rm tot} = 2.74$ [23]. Furthermore, the γ-ray detection efficiency at this γ-ray energy in our experiment was only ϵ_γ(80 keV) = 11.0(3)%; thus, at most 0.4 α–γ(80 keV) coincident events could be expected. This explains the non-observation of α(7347–7423 keV)–γ(80 keV) coincident decays in our experiment, if one assumes that the α decay of ^{179}Pb feeds the 80 keV excited state in ^{179}Hg.

However, the L- and a weaker M-internal conversion (the ratio $L/M = 4.3$ [23]) of this transition will produce conversion electrons with the energies of ∼65 keV (L conversion) and ∼74 keV (M conversion). Depending on the emission angle of these electrons, they will be either fully or partially registered in the PSSD. Thus, their energy will be fully or partially summed in the PSSD with the energy of the feeding α decay of ^{179}Pb. This will result in higher energy tail extending from the position of the 'unperturbed' α decay (α_0) up to the energy corresponding to the full α_0+e$^-$(L, M) summing peak. Within the energy resolution of the PSSD we are not able to distinguish the summing with the L and M conversion electrons, so we consider the highest energy events at 7420(20) keV as arising from this full-energy summing peak. Therefore, the energy of the unperturbed α decay of ^{179}Pb is estimated as 7350(20) keV, being the difference between the value of 7420 keV and the average value of the L and M conversion electron energies, which is ∼70 keV. As one can see from the inset to figure 1(a), the value of 7350(20) keV matches well the lowest energy events in the spectrum.

On these grounds we constructed the decay scheme of ^{179}Pb as shown in figure 4.

The reduced α-decay width, δ^2_α(7350 keV) = 33^{+14}_{-10} keV, was calculated for this decay with the Rasmussen prescription [20] with an assumption of $\Delta L = 0$. This value is similar to the reduced α-decay width of 54(8) keV for the neighboring even–even isotope ^{180}Pb [7], which suggests that the 7350 keV decay is unhindered. Therefore, based on the presumed assignment of $I^\pi = (9/2^-)$ for the excited state at 80 keV and unhindered 7350 keV decay, we assign $I^\pi = (9/2^-)$ to the ground state of ^{179}Pb.

As extensively discussed in [14, 22], the $7/2^-$ ground state of ^{175,177}Hg can be understood as being due to an odd neutron occupying a somewhat mixed $7/2^-$ state from $f_{7/2}$ or $h_{9/2}$ orbitals at a weak deformation of $\beta_2 \sim 0.1$. The excited $9/2^-$ level in these nuclei is then understood as due to the occupation of the spherical $h_{9/2}$ orbital. Therefore, the ground state of ^{179}Pb is most likely also based on the spherical $h_{9/2}$ orbital. In this respect it is valuable to note that the recent charge radii measurements of the isotopes $^{182-190}$Pb [2–4] showed a small deviation from the predictions of the spherical liquid drop model in the vicinity of the neutron mid-shell at $N = 104$ (^{186}Pb), see figure 3 of [2]. However, as discussed in [2, 3], these

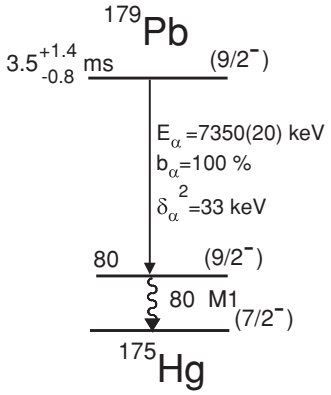

Figure 4. Decay scheme for ^{179}Pb proposed in our work. The $9/2^-$ state at 80 keV in ^{175}Hg is taken from [14]. All I^π assignments are tentative and shown in brackets. See the text for details.

deviations can be explained without the introduction of a static deformation. Moreover, by moving beyond the mid-shell at $N = 104$, the deviation from the spherical liquid drop model predictions become less, as demonstrated by the measured charge radii of ^{182,183}Pb. This also suggests that the ground state of ^{179}Pb should be spherical.

Related to the above discussion, we note that the direct 7430(20) keV α decay to the presumed $7/2^-$ ground state of ^{175}Hg should be strongly hindered as it would involve different parent and daughter configurations. An upper limit of $\delta^2_\alpha(7430\ \text{keV}) \leqslant 2(1)$ keV can be deduced by assuming that one event in the vicinity of this energy in the inset to figure 1(a) is due to the 7430 keV decay. This would result in a lower limit for the hindrance factor value of HF $\geqslant$16(8) for this decay relative to the unhindered 7350(20) keV decay. This situation is also similar to the case of ^{181}Pb [7].

4.2. $^{179}Tl^m$ decay chain

So far, none of the spin and parity values in the α-decay chain of ^{179}Tl^m to its daughter nuclide ^{167}Re have been experimentally established. Therefore, all the I^π values quoted in the literature and shown in figure 3 are tentative and are based on the systematics of excited states and α-decay hindrance factor values as discussed below.

Our new half-life and α-decay branching ratio data allowed us to deduce more precise reduced α-decay widths for ^{179}Tl^m, ^{175}Au^m and ^{171}Ir^m, see figure 3. All the δ^2_α values of these nuclides are in the unhindered range of $\sim$50–90 keV. Therefore, the respective α decays must connect states with same spin, parity and configuration. Thus, based on both the most probable assignment of $I^\pi = 11/2^-$ for the state at 92+Δ keV in ^{167}Re [1] and on an unhindered character of the α decays connecting the nuclei in the decay chain of ^{179}Tl^m, we assign $I^\pi = 11/2^-$ to the α-decaying isomers ^{171}Ir^m, ^{175}Au^m and ^{179}Tl^m, see figure 3. The $11/2^-$ assignment for ^{175}Au^m was also suggested in a recent in-beam work [19].

Thus, our detailed data support the suggestion of the study [17] that the proton $1h_{11/2}$ orbital becomes responsible for the short-lived α-decaying isomer in ^{179}Tl. In the heavier odd-A isotopes $^{181-201}$Tl, the $9/2^-$ proton intruder states are well known and their excitation energies follow a well-established parabolic energy dependence on the neutron number, with a minimum in the vicinity of the neutron mid-shell at $N = 104$, see e.g. figure 5 of our recent study [24]. As discussed in [24], by extrapolating this trend to lighter Tl isotopes, the $9/2^-$

state in ^{179}Tl is expected at an excitation energy of ∼1170 keV; thus, it should be well above the $11/2^-$ state. This mechanism naturally explains both the presence of an $11/2^-$ isomer in ^{179}Tl and the absence of the $9/2^-$ isomeric state. Consistent with this, a $I^\pi = 11/2^-$ assignment was suggested for the short-lived isomeric state in ^{177}Tl at $E^* = 807(18)$ keV decaying by both proton and α emission [13, 25].

We note that the value of $\delta^2_\alpha(^{179}\mathrm{Tl}^m) = 89(4)$ keV is ∼30% larger than the reduced α widths of $^{175}\mathrm{Au}^m$ and $^{171}\mathrm{Ir}^m$. A possible explanation for this effect could be a sizable proton decay and/or an internal transition branch from this state, which would reduce the reduced width $\delta^2_\alpha(^{179}\mathrm{Tl}^m)$. For example, the $(11/2^-)$ isomer in ^{177}Tl has an ∼50% proton-decay branch [13, 25]; thus, a possible proton branch cannot be excluded in $^{179}\mathrm{Tl}^m$ as well. However, no proton decay or internal transition branches were found in our analysis of $^{179}\mathrm{Tl}^m$: thus, this question still remains open.

Finally, a comment on the β^+/EC-decay branch of $^{175}\mathrm{Au}^m$ is in order here, see figure 3. Clearly, the direct decay between the presumable $(11/2^-)$ state of $^{175}\mathrm{Au}^m$ and the $(7/2^-)$ state of ^{175}Pt should be strongly hindered, as it would be the second-forbidden decay. Therefore, we have to assume that this decay proceeds via excited states in ^{175}Pt, e.g. by the first-forbidden decay toward the known $13/2^+$ and/or $11/2^+$ states in ^{175}Pt [26] or, even more probable, toward the yet unknown $9/2^-$ and/or $11/2^-$ excited states which are expected to occur in this nucleus. That is why the β^+/EC-decay branch of $^{175}\mathrm{Au}^m$ is shown in figure 3 as feeding toward an excited state in ^{175}Pt, which is meant to represent such excited state(s).

5. Conclusions

The α-decay study of the new isotope ^{179}Pb was performed in the complete fusion reaction of ^{40}Ca ions with the ^{144}Sm target. An $I^\pi = 9/2^-$ spin-parity assignment for ^{179}Pb is suggested, which is based on the spherical $1h_{9/2}$ neutron configuration.

For the first time, a detailed study of the full decay sequence $^{179}\mathrm{Tl}^m \rightarrow {}^{175}\mathrm{Au}^m \rightarrow {}^{171}\mathrm{Ir}^m \rightarrow {}^{167}$Re was performed. The unhindered nature of the α decays within the chain confirmed the presence of $11/2^-$ states in all these nuclei. The excitation energies of these states relative to the ground states in ^{179}Tl, ^{175}Au and in ^{171}Ir still remains unknown.

Acknowledgments

We thank the UNILAC staff for providing the stable and high-intensity ^{40}Ca beams. This work was supported by FWO-Vlaanderen (Belgium), GOA/2004/03 (BOF-KU Leuven) and the 'Interuniversity Attraction Poles Programme—Belgian State Belgian Science Policy' (BriX network P6/23), by the European Commission within the Sixth Framework Programme through I3-EURONS (Contract RII3-CT-2004-506065) and by the UK Science and Technology Facilities Council. S Antalic and Š Šáro were supported by the Slovak Research and Development Agency under contract no APVV-20-006205.

References

[1] Evaluated Nuclear Structure Data File (ENSDF) http://www.nndc.bnl.gov/ensdf/
[2] Seliverstov M D *et al* 2009 *Eur. Phys. J.* A **41** 315
[3] De Witte H *et al* 2007 *Phys. Rev. Lett.* **98** 112502
[4] Sauvage J *et al* 2009 *Eur. Phys. J.* A **39** 33
[5] Firestone R B *et al* 1996 *Table of Isotopes* 8th edn (New York, Chicester, Brisbane, Toronto, Singapore: Wiley)
[6] Carpenter M P, Kondev F G and Janssens R V F 2005 *J. Phys. G: Nucl. Part. Phys.* **31** S1599

[7] Andreyev A N *et al* 2009 *Phys. Rev.* C **80** 054322
[8] Münzenberg G *et al* 1979 *Nucl. Instrum. Methods* **161** 65
[9] Hofmann S *et al* 1979 *Z. Phys.* A **291** 53
Hofmann S and Münzenberg G 2000 *Rev. Mod. Phys.* **72** 733
[10] Andreyev A N *et al* 2004 *Nucl. Instrum. Methods* A **533** 409
[11] Saro S *et al* 1996 *Nucl. Instrum. Methods* A **381** 520
[12] Schneider J R H 1984 *PhD Thesis* GSI report, GSI-84-3 (unpublished)
[13] Poli G L *et al* 1999 *Phys. Rev.* C **59** R2979
[14] O'Donnell D *et al* 2009 *Phys. Rev.* C **79** 051304(R)
[15] Schneider J R H *et al* 1983 *Z. Phys.* A **312** 21
[16] Page R D *et al* 1996 *Phys. Rev.* C **53** 660
[17] Toth K S *et al* 1998 *Phys. Rev.* C **58** 1310
[18] Rowe M W *et al* 2009 *Phys. Rev.* C **65** 054310
[19] Kondev F G *et al* 2001 *Phys. Lett.* B **512** 268
[20] Rasmussen J O 1959 *Phys. Rev.* **113** 1593
[21] Andreyev A N *et al* 2009 to be published
[22] Melerangi A *et al* 2003 *Phys. Rev.* C **68** 041301(R)
[23] Kibédi T *et al* 2008 *Nucl. Instrum. Methods* A **589** 202
Conversion coefficients calculator BrIcc v2.2a http://wwwrsphysse.anu.edu.au/nuclear/bricc/
[24] Andreyev A N *et al* 2009 *Phys. Rev.* C **80** 024302
[25] Kettunen H *et al* 2004 *Phys. Rev.* C **69** 054323
[26] Cederwall B *et al* 1990 *Z. Phys.* A **337** 283